Table III—Comparison of Effect of Equimolar Concentrations of *N*-Benzoyl Amino Acids and Amino Acid Analogs on Growth of *L. casei* 7469 [a]

N-Benzoyl Derivative	Inhibition [b], %
DL-Allylglycine	17
p-Chloro-DL-phenylalanine	94
o-Fluoro-DL-phenylalanine	82
m-Fluoro-DL-phenylalanine	97
p-Fluoro-DL-phenylalanine	72
β-Hydroxy-DL-norleucine A	14
β-Hydroxy-DL-norleucine B	22
L-Leucine	23
DL-Methionine	20
L-Methionine	18
p-Nitro-L-phenylalanine	78
DL-Norleucine	47
DL-Norvaline	13
L-Phenylalanine	39
β-2-Thienyl-DL-alanine	76
β-3-Thienyl-DL-alanine	56
L-Tryptophan	74
L-Tyrosine ethyl ester	26
L-Valine	16

[a] Maximum growth in inoculated control tube (containing no test compound) was 166–173 Klett units. For explanation of extent of variation of values, see footnote to Table II. [b] Concentration was 4.47 μmoles/ml and was the final concentration in the assay system. For details of assay, see Ref. 1.

nisms of inhibition of these compounds could be dissimilar. Certain tumor systems, as well as bacterial and mammalian asparaginase and glutamine synthetase, are inhibited by carbobenzoxy, phenacetyl, and phenylpropionyl amino acids (13–15).

Most compounds exhibiting notable inhibitory activity in the present studies were benzoyl derivatives of phenylalanine analogs. Therefore, it will be interesting to test the activity of these compounds against melanomas, wherein the phenylalanine metabolism is believed to be intimately involved. In view of the effect of similar compounds on mammalian tumor systems and certain isolated enzyme systems (13–15), the study of the activity of the compounds in asparaginase-sensitive tumors is also indicated.

REFERENCES

(1) T. T. Otani, *Cancer Chemother. Rep.*, **38**, 25 (1964).

(2) T. T. Otani and M. R. Briley, *J. Pharm. Sci.*, **67**, 520 (1978).

(3) *Ibid.*, **68**, 496 (1979).

(4) M. D. Armstrong and J. D. Lewis, *J. Biol. Chem.* **188**, 91 (1951).

(5) V. du Vigneaud, H. McKennish, Jr., S. Simmonds, K. Dittmer, and G. B. Brown, *ibid.*, **159**, 385 (1945).

(6) R. G. Garst, E. Campaigne, and H. G. Day, *ibid.*, **180**, 1013 (1949).

(7) M. F. Ferger and V. du Vigneaud, *ibid.*, **179**, 61 (1949).

(8) T. T. Otani and M. Winitz, *Arch. Biochem. Biophys.*, **102**, 464 (1963).

(9) T. T. Otani and M. R. Briley, *J. Pharm. Sci.*, **65**, 534 (1976).

(10) J. P. Greenstein and M. Winitz, in "Chemistry of the Amino Acids," Wiley, New York, N.Y., 1961.

(11) D. D. Van Slyke, *J. Biol. Chem.*, **83**, 425 (1929).

(12) G. E. Foley, R. E. McCarthy, V. M. Binns, E. E. Snell, B. M. Guirard, G. W. Kidder, V. C. Dewey, and P. S. Thayer, *Ann. N. Y. Acad. Sci.*, **76**, 413 (1958).

(13) N. Lustig, H. Spiegelstein-Klarfeld, E. Schneider, and N. Lichenstein, *Isr. J. Chem.*, **12**, 757 (1974).

(14) H. Spiegelstein-Klarfeld, N. Lustig, and N. Lichenstein, *Experientia*, **30**, 1233 (1974).

(15) N. Lichenstein, N. Grossowicz, and M. Schlesinger, *Isr. J. Med. Sci.*, **13**, 316 (1977).

Degradation Kinetics of a New Cephalosporin Derivative in Aqueous Solution

ELISABETH S. RATTIE *, JAMES J. ZIMMERMAN ‡, and LOUIS J. RAVIN *x

Received December 8, 1978, from the **Research and Development Division, Smith Kline and French Laboratories, Philadelphia, PA 19101,* and the ‡*Department of Pharmaceutics, School of Pharmacy, Temple University, Philadelphia, PA 19140.* Accepted for publication May 8, 1979.

Abstract □ The degradation kinetics of a new cephalosporin derivative (I) in aqueous solution were investigated at 60°, $\mu = 0.5$, at pH 2.0–10.0. The observed degradation rates followed pseudo-first-order kinetics and were influenced significantly by H_2O and OH^- catalysis. No primary salt effect was observed in the acid region, but a positive salt effect was observed at pH 9.4. A general base catalytic effect by a phosphate buffer species was observed at pH 7–8. The pH–rate profile for I exhibited a degradation minimum at pH 6.05. The Arrhenius activation energies determined at pH 4.0 and 9.4 were 27.2 and 24.5 kcal/mole, respectively. Excellent agreement between the theoretical pH–rate profile and the experimental data supported the hypothesized degradation process. A comparison of I and cefazolin revealed close structural and stability analogies.

Keyphrases □ Cephalosporins—derivatives, degradation kinetics, aqueous solution, compared to cefazolin □ Antibacterial agents—cephalosporin derivatives, degradation kinetics, aqueous solution, compared to cefazolin □ Pharmacokinetics—cephalosporin derivatives, degradation, aqueous solutions, compared to cefazolin

Yamana and Tsuji (1) reported the comparative stability of several commercially available cephalosporin derivatives including those with an α-amino group in their side chain (*e.g.*, cephalexin, cephradine, and cephaloglycin) and those lacking the side-chain α-amino group (*e.g.*, cephalothin, cephaloridine, and cefazolin). Cephalosporins possessing the α-amino group may be administered orally, and cephalexin and cephradine have the highest stability of the derivatives investigated. Cephalosporins lacking the α-amino group are not administered orally, and cefazolin in particular is very unstable in the acid pH region.

This report describes the stability kinetics of a new cephalosporin derivative, 3-[2-(5-methyl-1,3,4-thiadiazyl)mercaptomethyl]-7-[D-(−)-mandelamido]-3-cephem-4-carboxylic acid sodium salt (I) (Table I). Of the cephalosporin derivatives previously investigated (1), I most closely resembles cefazolin. These two compounds have the same R_2 group but different R_1 groups. The continued investigation of cefazolin-like derivatives appears to be warranted in view of the clinical advantages of cefazolin over other cephalosporins (2).

BACKGROUND

As a result of previous studies (1, 3), the following conclusions may be

0022-3549/79/1100-1369$01.00/0

Table I—Structural Comparisons between I and Cefazolin

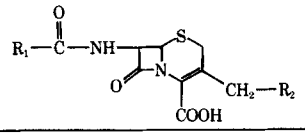

Cephalosporin	Substituents R_1	Substituents R_2	pKa
I	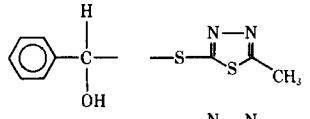		2.50[a]
Cefazolin	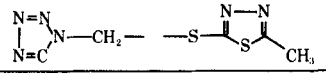		1.70, 2.54[b], 2.38[c]

[a] The pKa was determined spectrophotometrically and apparently refers to the carboxylic acid group (present study). [b] The pKa of 1.70 was determined kinetically and apparently refers to the thiadiazole moiety; pKa 2.54 was determined potentiometrically and refers to the carboxylic acid group (Ref. 1). [c] The pKa of 2.38 was determined potentiometrically at 60° (Ref. 10).

offered concerning the effect of substituent changes at R_1 on degradation rates of cephalosporin derivatives at various pH values:

1. Substituent changes at R_1 appear to have little effect on the rate constants for H^+- and OH^--catalyzed hydrolysis. Cephalothin and cephaloglycin with identical R_2 groups but different R_1 groups have nearly identical rate constants for H^+ and OH^- catalysis (1).

2. Substituent changes at R_1 may affect the shape of the pH profile in the neutral pH region. Thus, cephalosporins with an α-amino group at R_1 show a sharp rise in their pH profiles at pH 6.0–8.0, and they also show an inflection point at pH ~8.0 (1).

Furthermore, a comparison of the rate constants for substituted phenylcephalosporins reveals a 3.2-fold range in the rate constants for spontaneous hydrolysis. A similar comparison for the two phenyldeacetylcephalosporin derivatives shows no such change. In view of these structure–activity relationships, the effect, if any, of structural change at R_1 in I would be expected to appear in the neutral pH region.

EXPERIMENTAL

Materials—Compound I[1] was purified from acetic acid–water. All other chemicals were reagent grade. The water used for buffers was freshly distilled from a stainless steel still[2].

Buffer Solutions—The following buffers were used in the kinetic studies: hydrochloric acid–potassium chloride[3] (pH 2.0), citrate buffer (pH 3.0, 4.0, 5.0, and 5.5), phosphate buffer (pH 6.0, 6.5, 7.0, 7.5, and 8.0), and carbonate buffer (pH 9.4 and 10.0). They were freshly prepared by dissolving hydrochloric acid, citric acid, monobasic sodium phosphate, or sodium bicarbonate together with potassium chloride in distilled water and adjusting the pH with drops of concentrated sodium hydroxide. The pH readings were made using a research pH meter[4] equipped with a combination electrode[5].

The buffers were 0.1 *M* with respect to hydrochloric acid and citrate, phosphate, and carbonate ions (except when a buffer effect was investigated) and were adjusted to an ionic strength of 0.5 with potassium chloride except when primary salt effects were investigated.

Kinetic Procedure—Approximately 200 mg of I was accurately weighed and dissolved in 200 ml of appropriate buffer, which had been heated to 60° to produce a 1.99×10^{-3} *M* concentration. At this temperature, degradation proceeded at a rate convenient for analysis. The flasks were kept at 60° in a constant-temperature oil bath with a precision of ±0.1°[6].

Two 10-ml samples were withdrawn at appropriate intervals, which had been determined after preliminary studies. The samples were cooled in an ice bath and analyzed.

Analytical Procedure—Residual intact I was determined iodometrically using a procedure similar to that of Finholt *et al.* (4) for penicillin G. From the reaction solutions, two 10-ml samples, A and B, were pipetted into separate 125-ml erlenmeyer flasks. To A, 5 ml of 1 *N* NaOH was added. After the sample stood 15 min at room temperature, 5 ml of 1 *N* HCl, 20 ml of acetate buffer [35% (w/v) sodium acetate; 42.4% (v/v) acetic acid], and 25 ml of 0.02 *N* iodine[7] were added. To B, 20 ml of acetate buffer and 25 ml of 0.02 *N* iodine were added.

The flasks were stoppered and kept in darkness for 3.5 hr at room temperature. The excess iodine in both samples was then titrated with 0.025 *N* sodium thiosulfate using Thyodene as an indicator[8]. The difference between the two titration values gave the amount of iodine equivalent to the amount of I present. The iodine equivalence for I was calculated to be 12, and each milliliter of 0.02 *N* iodine was equivalent to 5.2 mg of I.

pKa Determination at 60°—The pKa of I was determined spectrophotometrically (5) using a spectrophotometer[9] with a thermostatically controlled cell compartment. Compound I was dissolved sequentially in a series of buffer solutions to a concentration of 0.08 mg/ml, and spectra were obtained between 240 and 400 nm. The buffers were: 0.1 *N* HCl; 0.1 *M* chloroacetic acid adjusted to pH 2.2, 2.4, 2.8, and 3.2; 0.1 *M* formic acid adjusted to pH 4.4; and 0.1 *M* phosphoric acid adjusted to pH 6.0. The adjustments were made with 0.1 *N* KOH at 60° on a research pH meter. Each solution of I yielded λ_{max} = 268 nm with an isosbestic point at 292 nm. Equation 1 was used to estimate a pKa = 2.50 for I at 268 nm:

$$\text{pKa} = \text{pH} + \log [(d_I - d)/(d - d_M)] \qquad \text{(Eq. 1)}$$

where d_I is the ionized species absorbance at pH 6.0, d_M is the nonionized species absorbance at pH 1.0, and d is the absorbance at intermediate pH.

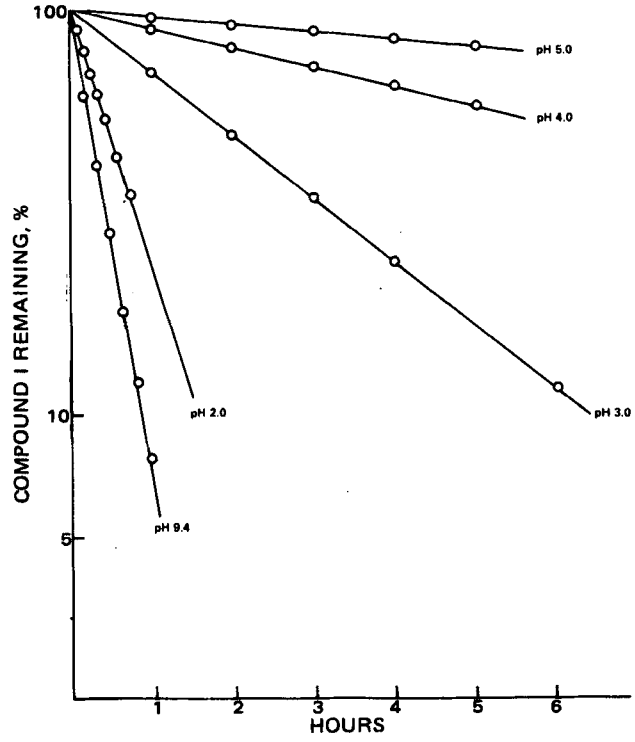

Figure 1—*Pseudo-first-order plots for the degradation of I at various pH values, 60°, and* $\mu \doteq 0.5$.

RESULTS AND DISCUSSION

Reaction Order and Observed Rate Constants—The degradation of I followed pseudo-first-order kinetics at constant pH, temperature, and ionic strength at pH 2.0–10.0. This result is shown by the linear log concentration *versus* time plots at 60° in Fig. 1. The pseudo-first-order rate constants, k_{obs}, for each pH value are given in Table II together with associated buffer species fractions, f. The number of half-lives over which the data were collected was 1–5 × $t_{1/2}$, depending on the pH.

[1] SK&F Laboratories, Philadelphia, Pa.
[2] Barnstead.
[3] The hydrochloric acid–potassium chloride buffer contained 5% *N,N*-dimethylacetamide to solubilize I below pH 3.0.
[4] Beckman Instruments.
[5] Fisher Scientific Co.
[6] Philadelphia Roto-Stat.
[7] Iodine, 0.1 *N*, Harleco.
[8] Standards were freshly prepared by appropriate dilution before each study.
[9] Cary model 15.

Table II—Observed Rate Constants for Degradation of I and Buffer Species Fractions, *f*, at 60° and $\mu = 0.5$

pH	Buffer System[a,b]	Species Fractions						k_{obs}, $min^{-1} \times 10^3$
		f_{H_3A}	$f_{H_2A^-}$	$f_{HA^{2-}}$	$f_{A^{3-}}$	f_{HA^-}	$f_{A^{2-}}$	
2.0	HCl/KCl	—	—	—	—	—	—	24.01
3.0	Citrate	0.333	0.635	0.032	—	—	—	5.96
4.0	Citrate	0.033	0.637	0.319	0.011	—	—	1.77
5.0	Citrate	—	0.130	0.650	0.220	—	—	0.647
5.5	Citrate	—	0.030	0.468	0.502	—	—	0.623
6.0	Phosphate	—	0.776	0.224	—	—	—	0.606
6.5	Phosphate	—	0.523	0.477	—	—	—	0.626
7.0	Phosphate	—	0.257	0.743	—	—	—	0.749
7.5	Phosphate	—	0.099	0.901	—	—	—	1.43
8.0	Phosphate	—	0.034	0.966	—	—	—	2.22
9.4	Carbonate	—	—	—	—	0.876	0.124	35.5
10.0	Carbonate	—	—	—	—	0.640	0.360	114.2

[a] The ionization constants for the citrate and phosphate buffers at 60° and $\mu = 0.5$ are from Ref. 4. For citric acid and citrate ions, $pK_1 = 2.72$, $pK_2 = 4.30$, and $pK_3 = 5.47$. For dihydrogen phosphate ion, $pK_2 = 6.54$. The ionization constant for bicarbonate ion at 60° and $\mu = 0.5$ is $pK_2 = 10.25$ from Ref. 11. [b] Buffer species fractions were calculated according to Ref. 12.

General Acid–Base Catalysis—The catalytic effects of buffer species for the citrate, phosphate, and carbonate buffers were investigated at constant pH, temperature, and ionic strength in solutions containing 1 mg of I/ml. For each buffer system, the rate constant, k_{obs}, was determined experimentally as a function of buffer concentrations of 0.05–0.2 *M*. The observed rate constants and corresponding buffer concentrations are given in Table III.

The results in Table III indicate that k_{obs} is independent of citrate buffer concentration at pH 3 and 4. Since the dominant citrate species in solution at these pH values are H_3A, H_2A^-, and HA^{2-} (Table I), these species may be disregarded as general acid–base catalysts. The citrate buffer effect was not investigated at pH 5.5, where the dominant species are HA^{2-} and A^{3-}, but A^{3-} also may be disregarded as a catalyst because of the close fit obtained for the pH–rate profile without it.

Figure 2 illustrates the variable effect of phosphate buffers on the degradation of I at pH 6.0–8.0. Based on Tables II and III, it is apparent that $H_2PO_4^-$ is the dominant species in solution at pH 6, where the rate constant is independent of buffer concentration, while HPO_4^{2-} is the dominant species in solution at pH 7.0 and 7.5, where the rate constant is increasingly dependent on buffer concentrations. These trends suggest that HPO_4^{2-} is a general base catalyst within the phosphate buffer region. An attempt to estimate the rate constant, $k_{HPO_4^{2-}}$, for the catalytic effect was based on:

$$k_{obs} = k_0 + k''[P] \qquad \text{(Eq. 2)}$$

where k_0 is the rate constant at zero buffer concentration, $[P]$ is the total buffer concentration, and:

$$k'' = (k_{HPO_4^{2-}})(f_{HPO_4^{2-}}) \qquad \text{(Eq. 3)}$$

where $f_{HPO_4^{2-}} = K_2/(a_{H^+} + K_2)$.

Table III—Effect of Buffer Concentration on the Pseudo-First-Order Rate Constants for I Degradation at 60° and $\mu = 0.5$

pH (Buffer)	k_{obs}, $min^{-1} \times 10^3$			
	0.05 *M*	0.10 *M*	0.15 *M*	0.20 *M*
3.0 (citrate)	6.43	5.96	—	6.00
4.0 (citrate)	1.80	1.77	1.73	—
6.0 (phosphate)	0.594	0.606	—	0.598
6.5 (phosphate)	0.686	0.626	—	0.643
7.0 (phosphate)	0.724	0.749	—	0.790
7.5 (phosphate)	1.18	1.43	—	1.92
8.0 (phosphate)	1.68	2.22	2.61	—
9.4 (carbonate)	—	35.5	35.7	37.8

Table IV—Values of k_0 and k'' Estimated from Eq. 3

pH	k_0, $min^{-1} \times 10^{3a}$	k'', $M^{-1}\ min^{-1} \times 10^{3b}$
6.0	0.599	—
6.5	0.626	—
7.0	0.703	0.437
7.5	0.932	4.97
8.0	1.48	9.28

[a] $k_0 = k_{obs}$ independent of buffer effects. [b] k'' = second-order rate constant for buffer effects.

Equation 3 predicts a zero intercept when k'' (Table IV) is plotted against $f_{HPO_4^{2-}}$ (Table II), but a plot of the appropriate values for these constants yielded a relatively large negative intercept ($-2.783 \times 10^{-2}\ M^{-1}\ min^{-1}$), which was significantly different from zero at the 80% confidence level. Furthermore, k'' should vary to the same extent as $f_{HPO_4^{2-}}$ when the pH is varied. This was not the case since the relative k'' values were 1, 11.4, and 21.2 at pH 7.0, 7.5, and 8.0, respectively, while the relative $f_{HPO_4^{2-}}$ values were 1.0, 1.2, and 1.3. Either HPO_4^{2-} is not the sole contributing catalytic species or its activity is far greater than predicted from its pKa.

Table III further indicates that k_{obs} is independent of the carbonate buffer concentration at pH 9.4. At this pH, HCO_3^- is the dominant species in solution (Table II) and may, therefore, be excluded as a general base catalyst.

Primary Salt Effect—The primary salt effect on the hydrolysis of I was studied at constant pH and temperature, but the ionic strength was varied with potassium chloride addition. Studies were conducted at pH 4.0 and 9.4 where general base catalysis was absent and secondary salt effects would be unimportant. The data at these pH values for ionic strength, μ, 0.3–1.0 are given in Table V.

Within restricted ranges of μ, plots of log k_{obs} *versus* $\sqrt{\mu}$ *or* $\sqrt{\mu}/(1 + \sqrt{\mu})$ should yield theoretical slopes equal to $2AZ_AZ_B$, where A is a constant for the solvent at a given temperature and Z_A and Z_B are the charges on reaction species A and B, respectively (6). While such plots would be expected to be linear only within limits of the Debye–Huckel expressions, Carstensen (7) recently reviewed kinetic salt effects in the pharmaceutical literature to show that plots utilizing $\sqrt{\mu}$ or $\sqrt{\mu}/(1 + \sqrt{\mu})$ may be linear with ionic strength ≥ 1.0. This author pointed out that the use of $\sqrt{\mu}/(1 + \sqrt{\mu})$ instead of $\sqrt{\mu}$ at higher ionic strengths more fre-

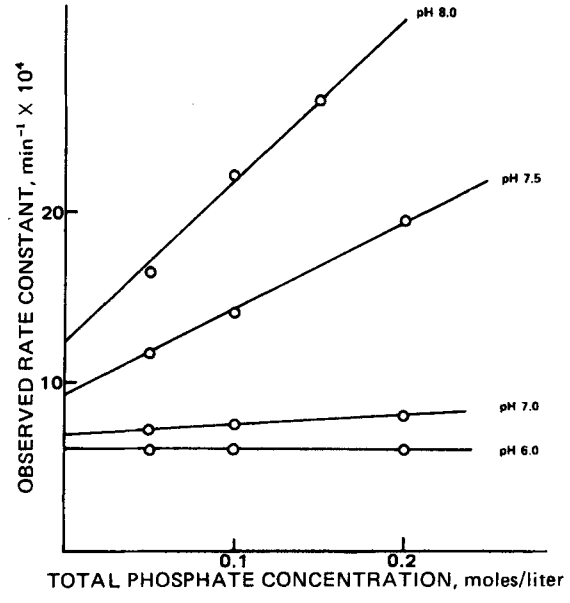

Figure 2—*Plots of* k_{obs} versus *the total phosphate buffer concentration for the degradation of I at various pH values, 60°, and* $\mu = 0.5$.

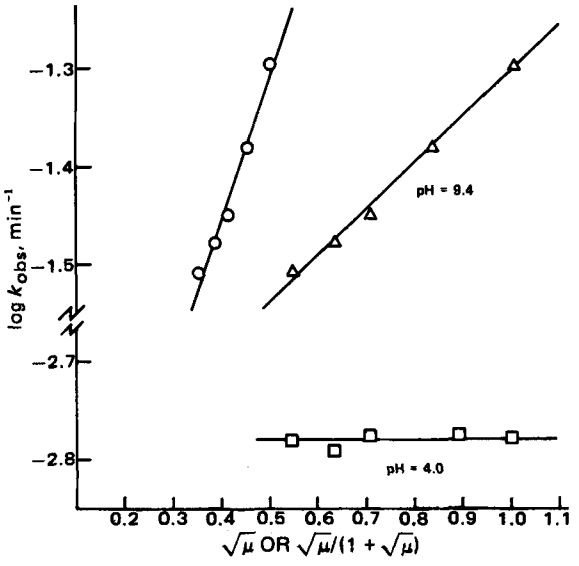

Figure 3—*Plots of log* k_{obs} versus $\sqrt{\mu}$ (△ *and* □) *or* $\sqrt{\mu}/(1+\sqrt{\mu})$ (○) *for the degradation of I at 60° and pH 4.0 and 9.4.*

quently produces values of $2AZ_AZ_B$ that are in agreement with theoretical values.

The data from Table V were used in preparing plots of log k_{obs} *versus* $\sqrt{\mu}$ and $\sqrt{\mu}/(1+\sqrt{\mu})$ in Fig. 3. A larger positive kinetic salt effect was obtained at pH 9.4 when the data were plotted with $\sqrt{\mu}/(1+\sqrt{\mu})$ than with $\sqrt{\mu}$, for which the slopes were 1.47 and 0.48, respectively. This result can be used as evidence for the reaction between two negatively charged species. By contrast, a kinetic salt effect was not observed at pH 4.0 (Fig. 3), and this result requires that at least one reactant be noncharged.

pH–Rate Profile—Values of log k_0 (*i.e.*, log k_{obs} independent of buffer effects) were plotted *versus* pH to yield the pH–rate profile for I (Fig. 4). In the absence of general base and intramolecular catalyses, the following specific acid–base reactions can be written for the hydrolysis of I, where HC stands for the nonionized form and C^- represents the ionized form:

$$HC + H^+ \xrightarrow{k_1} \text{products}$$
Scheme I

$$HC + H_2O \xrightarrow{k_2} \text{products}$$
Scheme II

$$HC + OH^- \xrightarrow{k_3} \text{products}$$
Scheme III

$$C^- + H^+ \xrightarrow{k_4} \text{products}$$
Scheme IV

$$C^- + H_2O \xrightarrow{k_5} \text{products}$$
Scheme V

$$C^- + OH^- \xrightarrow{k_6} \text{products}$$
Scheme VI

Of these reactions, Schemes II, V, and VI are sufficient to yield an excellent fit to the data as shown by the theoretical solid line in Fig. 4. The rate expressions associated with these reactions, expressed in terms of the total I concentration, [*a*], are:

$$-d[HC]/dt = k'_2 f_{HC}[a] \quad \text{(Eq. 4)}$$

$$-d[C^-]/dt = k'_5 f_{C^-}[a] \quad \text{(Eq. 5)}$$

$$d[C^-]/dt = k_6[OH^-]f_{C^-}[a] \quad \text{(Eq. 6)}$$

where $f_{HC} = a_{H^+}/(a_{H^+} + K_a)$, $f_{C^-} = K_a/(a_{H^+} + K_a)$, $k'_2 = k_2[H_2O]$, and $k'_5 = k_5[H_2O]$.

The overall rate is given as a sum of these reactions as expressed by:

$$-d[a]/dt = k_0[a] \quad \text{(Eq. 7)}$$

where:

$$k_0 = k'_2 f_{HC} + k'_5 f_{C^-} + k_6[OH^-]f_{C^-} \quad \text{(Eq. 8)}$$

Table V—Effect of Ionic Strength (μ) on Pseudo-First-Order Rate Constants for I Degradation at pH 4.0 and 9.4

μ	k_{obs}, min^{-1} × 10^3 pH 4.0	pH 9.4
0.3	1.66	31.1
0.4	1.62	33.3
0.5	1.79	35.5
0.7	—	41.6
0.8	1.80	—
1.0	1.71	50.7

Schemes II, V, and VI are compatible with the results of the ionic strength analysis. Thus, Scheme VI requires a positive kinetic salt effect (Fig. 3, pH 9.4) while Schemes II and V require a zero kinetic salt effect (Fig. 3, pH 4.0). The experimental slope of 1.47 at pH 9.4, however, is not in exact agreement with the theoretical value of 1.092 (7), and this disparity is not explained. These schemes also are compatible with the experimental slope values in the various regions of the pH–rate profile. Based on the data points at pH 8.0, 9.4, and 10.0, a slope of 0.95 is obtained compared with the theoretical value of 1.0 for Scheme VI. Within the plateau region, the zero slope is in agreement with that expected theoretically for Scheme V. From the data points at pH 2.0, 3.0, and 4.0, a slope value of −0.57 is obtained, which is intermediate to the theoretical extremes of −1.0 and 0 for Scheme II alone. This result is reasonable because of the variations in f_{HC} within this pH region (Eq. 4).

The exclusion of Schemes I, III, and IV from the analysis may be rationalized as follows. Scheme I would probably contribute a much greater negative component to pH 2.5–4.5 than the actual value of −0.57 since the theoretical slope = −2.0 when $K_a > a_{H^+}$ and provided that $k_1(a_{H^+})^2 > k_2 a_{H^+}$. Scheme I also predicts a slope of −1.0 when $a_{H^+} > K_a$ (pH < 2.5), but this low pH region was not investigated because of the low solubility of I below pH 2. Scheme III is potentially compatible with the plateau effect when $K_a > a_{H^+}$, but this reaction would require the unlikely value of $k_3 \approx 10^7$ ($K_3 = k_{obs} K_a/K_{w(exp)}$). Scheme IV was rejected on the basis of the ionic strength data since this reaction would require a negative kinetic salt effect at pH 4.0.

Estimates of k'_2, k'_5, and k_6 were obtained from a simultaneous solution of k_0 (Eq. 8) at pH 2.0, 6.0, and 10. The terms f_{HC} and f_{C^-} were calculated as described with $K_a = 3.162 \times 10^{-3}$ and $[OH^-]$ calculated according to:

$$[OH^-] = a_{OH^-}/\gamma_{\pm} \quad \text{(Eq. 9a)}$$

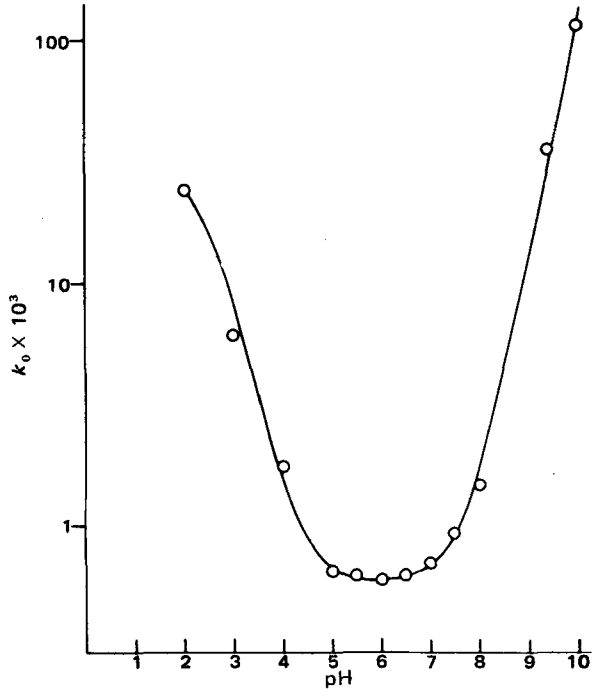

Figure 4—*Log* k_0*–pH profile for the degradation of I in aqueous solution at 60° and* $\mu = 0.5$. *The points are experimental values, and the solid line is the theoretical curve calculated from Eq. 8.*

Table VI—Rate Constants and Arrhenius Activation Parameters for I Degradation in Buffer Solutions at $\mu = 0.5$

pH	T	k_{obs}, $min^{-1} \times 10^3$	E_a, kcal/mole	log A, min^{-1}	$\Delta H^{\ddagger}$, kcal/mole	$\Delta S^{\ddagger}$, cal/deg/mole
4.0	35°	0.0624	27.2	15.1	—	—
	45°	0.277	—	—	—	—
	60°	1.77	—	—	—	—
9.4[a,b]	35°	1.77	24.5	14.6	23.8	−1.98
	45°	5.91	—	—	(11.9)	(13.9)
	60°	32.5	—	—	—	—

[a] Activation parameters calculated for 60° using the following equations: $k_{obs} = [(ekT/h)e^{\Delta S^{\ddagger}/R}e^{-E_a/RT}$, where $ek/h = 5.664 \times 10^{10}$ deg^{-1} sec^{-1} and $\Delta H^{\ddagger} = E_a - RT$ (13). [b] Values in parentheses are corrected values discussed in the text.

Table VII—Stability Comparisons between I and Cefazolin: $k_0 = k'_2 f_{HC} + k'_5 f_{C^-} + k_6[OH^-]f_{C^-}$ [a]

Parameter	I	Cefazolin	
k_0, min^{-1} (35° and $\mu = 0.5$)			
pH 4	6.24×10^{-5}	6.66×10^{-5} [b]	
pH 9.4	1.77×10^{-3}	1.03×10^{-3} [b]	
pH_{min}	6.05 (60°)	5.95 (35°)	5.51 (60°)[c]
E_a, kcal/mole	24.5 (pH 9.4)	28.5 (pH 10)	24.3 (pH 5.5)
$\Delta H^{\ddagger}$, kcal/mole[d]	11.9	14.8	11.7

[a] In Ref. 1, $k'_2 = k_a$, $k'_5 = k_0$, and $k_0 = k_{pH}$. [b] Values for cefazolin were computed from rate constants given in Table III of Ref. 1. [c] Data for cefazolin are from Ref. 10. [d] Values for the enthalpy of activation are corrected for the heat of ionization of water.

$$[OH^-] = K_{w(exp)}/a_{H^+}\gamma_{\pm} \quad \text{(Eq. 9b)}$$

where $K_{w(exp)} = a_{H^+}a_{OH^-} = 9.614 \times 10^{-14}$ and $\gamma_{\pm}$ = mean ionic activity coefficient product of water = 0.70, both at 60° and $\mu = 0.5$ (8). The resulting rate constants were: $k'_2 = 3.14 \times 10^{-2}$ min^{-1}, $k'_5 = 5.78 \times 10^{-4}$ min^{-1}, and $k_6 = 82.7$ M^{-1} min^{-1}. These constants, together with the K_a, $[OH^-]$, and a_{H^+} values, were used in the expression for k_0 to generate the theoretical profile in Fig. 4.

A theoretical pH minimum for the degradation of I was obtained by taking the derivative of Eq. 10 with respect to a_{H^+}, equating it to zero, and making appropriate substitutions:

$$k_0 = k'_2 f_{HC} + k_6 f_{C^-} \quad \text{(Eq. 10)}$$

The contribution from $k'_5 f_{C^-}$ was omitted from Eq. 10 since $dk_0/da_{H^+} = 0$ within the plateau region. The derivative equation is given by:

$$a_{H^+(min)} = [k_6 K_{w(exp)}/k'_2][1 + \sqrt{(1 + k'_2 K_a)/k_6 K_{w(exp)}}] \quad \text{(Eq. 11)}$$

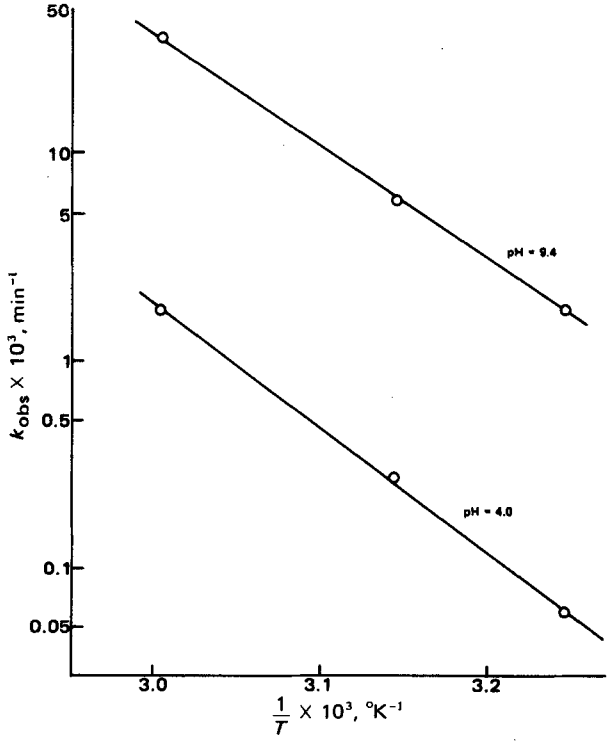

Figure 5—*Arrhenius plots for the degradation of I at $\mu = 0.5$ and pH 4.0 and 9.4.*

from which $a_{H^+(min)} = 8.948 \times 10^{-1}$ and $pH_{min} = 6.05$ may be calculated.

Micelle Formation—Since penicillin G forms micelles (9), which affect the kinetic data, I was investigated also for its ability to form micelles. High-resolution NMR was used to determine the possibility of micelle formation in 1, 10, and 30% aqueous I solutions (D_2O) at 60°. Spectra before and after the addition of deuterated methanol were identical. No micelle formation could be demonstrated.

Temperature Effect—The effect of temperature on the degradation of I was determined by measuring the degradation rates at 35, 45, and 60° in buffered solutions and $\mu = 0.5$. These measurements were made at pH 4.0 and 9.4. The values of k_{obs}, E_a, log A, and the enthalpies and entropies of activation are given in Table VI. The corresponding Arrhenius plots are shown in Fig. 5.

The Arrhenius parameters at pH 4.0 and 9.4 were very similar. Activation parameters were not computed at pH 4.0, where more than one reaction (Schemes II and V) apparently contributes significantly. However, activation parameters were calculated at pH 9.4 where Scheme VI is probably the dominant reaction. At this pH value, $k_{obs} = k_6[OH^-]$ and $\Delta S^{\ddagger}$ is given by:

$$\Delta S^{\ddagger}_{obs} = 1.9872\{\ln k_6 + \ln [OH^-] - \ln (ekT/h) + E_a/RT\} \quad \text{(Eq. 12)}$$

To obtain the entropy of activation independent of pH effects, the quantity 1.9872 ln $[OH^-]$ must be subtracted from the value of $\Delta S^{\ddagger}_{obs}$. Similarly, the calculated value of $\Delta H^{\ddagger}_{obs}$ includes the heat of ionization of water, which equals 11.9 kcal at 60° (8). This value must be subtracted from the overall enthalpy of activation to obtain the net value for the specific degradation reaction (Scheme VI). These corrected values of the entropy and enthalpy activations are given in parentheses in Table VI.

Comparative Stability—Based on Tables I and VI, there are close structural and stability analogies between I and cefazolin (Table VII). The structural difference at R_1 apparently is sufficient to alter the solubility such that cefazolin degradation can be followed kinetically below pH 1 at 5×10^{-3} M while I has a lower pH limit of 2.0 at 1.99×10^{-3} M. Consequently, a pKa of 1.70, probably associated with the thiadiazole moiety, was determined kinetically for cefazolin, but an analogous constant could not be determined for I (Table I).

It is apparent from Table VI that the data for both compounds fit the same kinetic expression for k_0. Indeed, the pH profile for cefazolin (1) is similar to that for I. The values of k_0 (35° and $\mu = 0.5$) for these two compounds were nearly identical at pH 4 and were similar at pH 9.4. The primary kinetic difference between cefazolin and I lies in the ionizable group affecting the degradation in the acid pH region. For cefazolin, a group with pKa 1.70 is required to fit the experimental data; for I, a group with pKa 2.50 is required. In attempting to fit the experimental data for I using pKa 1.70, the theoretical profile deviated excessively from k_0 at pH 3 and 4.

Further closeness in the degradation kinetics of the two compounds was manifested in pH_{min} similarities. Finally, their energies and enthalpies of activation are similar. Nevertheless, the enthalpy of acti-

vation for I was ~3 kcal/mole less than that of cefazolin. This difference was manifested in the larger k_0 value at pH 9.4 for I. The results of this study are in agreement with expected effects of structural changes at R_1 on the pH–rate profiles of cephalosporin derivatives.

REFERENCES

(1) T. Yamana and A. Tsuji, *J. Pharm. Sci.*, **65**, 1563 (1976).

(2) C. H. Nightingale, D. S. Greene, and R. Quintiliani, *ibid.*, **64**, 1899 (1975).

(3) J. M. Indelicato, T. T. Norvilas, W. J. Wheeler, and W. L. Wilham, *J. Med. Chem.*, **17**, 523 (1974).

(4) P. Finholt, G. Jurgensen, and H. Kristiansen, *J. Pharm. Sci.*, **54**, 387 (1965).

(5) A. Albert and E. P. Serjeant, "The Determination of Ionization Constants," 2nd ed., Barnes and Noble, New York, N.Y., 1971, chap. 4.

(6) A. Frost and R. Pearson, "Kinetics and Mechanisms," 2nd ed., Wiley, New York, N.Y., 1971, chap. 7.

(7) J. T. Carstensen, *J. Pharm. Sci.*, **59**, 1140 (1970).

(8) H. S. Harned and W. J. Hamer, *J. Am. Chem. Soc.*, **55**, 2194 (1933).

(9) J. T. Ong and H. B. Kostenbauder, *J. Pharm. Sci.*, **64**, 1379 (1975).

(10) E. S. Rattie, D. E. Guttman, and L. J. Ravin, *Arzneim.-Forsch. Drug Res.*, **28**, 6, 944 (1978).

(11) Landholt-Bornstein, *Physikalisch-Chemische Tabellen*, 5. Auflage, 2. Ergänzungsband.

(12) P. J. Niebergall, *Am. J. Pharm.*, **138**, 232 (1966).

(13) K. J. Laidler, "Chemical Kinetics," 2nd ed., McGraw-Hill, New York, N.Y., 1965, p. 88.

ACKNOWLEDGMENTS

Abstracted in part from a dissertation submitted by E. S. Rattie to the Graduate School, Temple University, in partial fulfillment of the Master of Science degree requirements.

Fluorometric High-Pressure Liquid Chromatographic Determination of Hydrocortisone in Human Plasma

THOMAS J. GOEHL ˣ, GLORIA M. SUNDARESAN, and VADLAMANI K. PRASAD

Received February 28, 1979, from the *Division of Biopharmaceutics, Food and Drug Administration, Washington, DC 20204.* Accepted for publication May 8, 1979.

Abstract □ A highly sensitive and specific method for hydrocortisone determination in plasma is described. In this method, an internal standard (Δ^4-pregnen-17α,20α,21-triol-3,11-dione) was added to plasma, which was then extracted with a mixture of methylene chloride–ether (60:40). After separation and evaporation of the organic phase, derivatization was carried out with dansylhydrazine. Upon completion of the reaction, the excess dansylhydrazine was reacted with pyruvic acid and a second extraction and evaporation step was performed. The residue was taken up in 100 μl of the high-pressure liquid chromatographic mobile phase, and 5 μl was injected onto a microparticulate silica column. Elution was carried out with an ethylene dichloride–butanol–water (91:8.5:0.5) mobile phase. The effluent was monitored with a fluorescence detector (excitation 240 nm; emission 470-nm cutoff filter). A linear calibration curve was found from 5 to 150 ng/ml with the precision estimated to be ±7% (*CV*).

Keyphrases □ Hydrocortisone—analysis, high-pressure liquid chromatography, fluorometry, plasma, humans □ Glucocorticoids—hydrocortisone, high-pressure liquid chromatographic and fluorometric analysis, plasma, humans □ High-pressure liquid chromatography—analysis, hydrocortisone, human plasma, fluorometry

Hydrocortisone is a potent anti-inflammatory, immunosuppressive, and antiallergenic drug (1). Since the discovery of hydrocortisone, numerous synthetic glucocorticoids have been prepared. However, hydrocortisone remains an important agent in modern adrenocorticoid steroid therapy.

Various analytical methods have been used to assay hydrocortisone in plasma including fluorescence (2, 3), competitive protein binding (4), enzyme immunoassay (5), and radioimmunoassay (6). All of these methods have problems with specificity. More recently, high-pressure liquid chromatographic (HPLC) methods for hydrocortisone assay in plasma have appeared (7–10). Most HPLC methods exhibit the required specificity but do not provide the low nanogram per milliliter sensitivity needed for bioequivalence studies. This paper describes a highly sensitive and specific HPLC assay for plasma hydrocortisone that can be used in bioequivalence studies.

EXPERIMENTAL

Apparatus—The modular high-performance liquid chromatograph consisted of a constant-flow pump[1], a valve-type injector[2], a fluorescence detector[3] (excitation 240 nm; emission 470-nm cutoff filter), and a strip-chart recorder[4] (0.5 cm/min). A stainless steel column (4.6 mm i.d. × 250 mm) packed with fully porous, irregularly shaped 5-μm silica[5] was obtained commercially.

Chromatographic Conditions—The mobile phase was ethylene dichloride–butanol–water (91:8.5:0.5). A flow rate of 1.5 ml/min was established (2200 psig), and the column was equilibrated for 16 hr. The column was maintained at 19.5° by inserting it into a glass sleeve, which was immersed in a constant-temperature water bath[6].

Reagents and Materials—Hydrocortisone[7], Δ^4-pregnen-17α,-20α,21-triol-3,11-dione[7] (internal standard), pyruvic acid[8], and dansylhydrazine[9] were obtained from commercial sources. All were used as received except dansylhydrazine, which was recrystallized from chloroform prior to use. Solvents used were spectroanalyzed ethylene dichloride[8], HPLC-grade butanol, methylene chloride, and ether[10]. All other materials were reagent grade.

[1] Chromatography pump, model M6000A, Waters Associates, Milford, Mass.
[2] Sample injection valve, model U6K, Waters Associates, Milford, Mass.
[3] Model FS970, Schoeffel Instruments, Westwood, N.J.
[4] Model 9176, Varian Instruments, Palo Alto, Calif.
[5] Prepacked Hibar II column with Lichrosorb SI-60 5-μm silica, Applied Science Laboratories, State College, Pa.
[6] Model 3080, Lab-Line Instruments, Melrose Park, Ill.
[7] Sigma Chemical Co., St. Louis, Mo.
[8] Fisher Scientific Co., Pittsburgh, Pa.
[9] Regis Chemical Co., Morton Grove, Ill.
[10] Burdick & Jackson Laboratories, Muskegon, Mich.

0022-3549/79/1100-1374$01.00/0